# 博 士 論 文

---

Epithelial-mesenchymal transition in oral cancer cells induced by chronic *Fusobacterium nucleatum* infection

*Fusobacterium nucleatum*の慢性感染による口腔癌細胞の上皮間葉転換

---

令和 6 年 3 月 25 日申請

北海道大学

大学院歯学院口腔医学専攻

中野　晋太郎

**Epithelial-mesenchymal transition in oral cancer cells induced by chronic *Fusobacterium nucleatum* infection**

Running title: *F. nucleatum*-induced EMT in oral cancer cells

Keyword: Oral cavity cancer, Fusobacterium nucleatum, Epithelial-mesenchymal transition (EMT), dexamethasone.

Author: Shintaro Nakano [a,b]

a) Department of Oral and Maxillofacial Surgery, Faculty of Dental Medicine and Graduate School of Dental Medicine, Hokkaido University, North 13 West 7, Kita-ku, Sapporo, Japan

b) Department of Oral Diagnosis and Medicine, Faculty of Dental Medicine and Graduate School of Dental Medicine, Hokkaido University, North 13 West 7, Kita-ku, Sapporo, Japan

**Abstract**

**Objectives**: Although several studies have reported the effects of *Fusobacterium nucleatum* infection in oral cancer cells, the cell infection period ranges from three days to a maximum of eight days. Therefore, the in vitro studies conducted to date may not be enough to mimic the environment of oral cancer, which involves constant exposure to oral commensal bacteria. This study aimed to elucidate the effects of chronic *Fusobacterium nucleatum* infection on oral cancer cells.

**Methods**: Human tongue squamous cell carcinoma cells were infected with *Fusobacterium nucleatum* for a 4-week period, and cells at 4-week, 2-week, and no infection were used in the experiments.

**Results**: Chronic *Fusobacterium nucleatum* infection increased the proliferative, invasive, and migratory capacities, decreased the expression of epithelial markers, and increased the expression of mesenchymal markers in cells in a time-dependent manner. In addition, the cells adapted to a slender and elongated morphology, and cell-to-cell separation was induced, suggesting that epithelial-mesenchymal transition occurs in a time-dependent manner. Furthermore, the mRNA level of CD44, a cancer stem cell marker, was upregulated in a time-dependent manner. However, when the cells were infected with *Fusobacterium nucleatum* for four weeks in the presence of dexamethasone, the epithelial-mesenchymal transition induced by *Fusobacterium nucleatum* infection was inhibited.

**Conclusions**: Epithelial-mesenchymal transition in human tongue squamous cell carcinoma cells was induced in a time-dependent manner by chronic *Fusobacterium nucleatum* infection and was inhibited by dexamethasone. Routine decontamination of the oral cavity may be crucial for controlling tumor invasion and metastasis.

## 1. Introduction

In 2018, 354,864 new cases of oral cancer were reported, accounting for 2 % of all malignancies. The prognosis for oral cavity cancer is poor, with a 5-year survival rate of approximately 50–60 % and 177,384 deaths in the same year [1].

Epithelial-mesenchymal transition (EMT) is a process in which epithelial cells lose cell polarity and intercellular adhesion and transform into mesenchymal-like cells, resulting in increased migration and invasive capacity, which promote tumor growth and metastasis, thereby worsening cancer prognosis [2]. Therefore, it is desirable to inhibit EMT induction to improve the survival prognosis in oral cancer.

Recently, the association between *Fusobacterium nucleatum* (*Fn)* and malignant tumors has been reported in large numbers, particularly in colon [3], stomach [4], pancreatic [5], and oral cavity cancers. *Fn* is an oral commensal anaerobic Gram-negative rod responsible for various dental infections including periodontitis. [6]. Several studies have reported that *Fn* is detected significantly more frequently in individuals with oral squamous cell carcinoma than in healthy individuals [7,8]. Moreover, since chronic inflammation causes cell cycle arrest, cytoplasmic distention, and chromatin fragmentation [9] and is closely associated with cancer development, *Fn* may aggravate oral carcinogenesis and cancer progression [10,11]. Recently, several studies have reported that *Fn* infection induces EMT in colon cancer cells and its underlying mechanisms [12–17], whereas, only a few studies have reported that infection with oral commensal bacteria induces EMT in oral cancer cells. Although several studies have reported the effects of oral microorganisms on EMT in oral cancer cells, the cell infection period only ranged from three days to a maximum of eight days [18–22]. Therefore, these in vitro

studies conducted to date may not be enough to mimic the environment of oral cancer, which involves constant exposure to oral commensal bacteria.

In this study, we investigated the effects of chronic *Fn* infection on oral cancer cells and EMT.

## 2. Material and Methods

### 2.1 Cell line and cell culture

HSC-3 cells (JCRB0623, human tongue squamous cell carcinoma) were provided by the National Institutes of Biomedical Innovation, Health, and Nutrition (JCRB Cell Bank, Osaka, JP). HSC-3 cells were cultured in minimum essential medium (MEM; Sigma-Aldrich, St. Louis, US) containing 10 % heat-inactivated fetal bovine serum (FBS; Cell Culture Technologies, Gravesano, Switzerland), 100 U/mL penicillin and 100 mg/mL streptomycin (MEM complete) at 37 ℃ with 5 % $CO_2$.

### 2.2 Bacteria strain and growth condition

*Fn* strain ATCC10953 (American Type Culture Collection, Manassas, VA, US) was cultured anaerobically (85 % $N_2$, 10 % $H_2$, 5 %$CO_2$) at 37 ℃ in Brain Heart Infusion broth (Becton Dickinson, Franklin Lakes, US), supplemented with hemin (5 μg/mL), and menadione (1 μg/mL), for 24 h, and stored in a -70 ℃ freezer until just before use.

### 2.3 Establishment of the infection model

To mimic chronic inflammation caused by *Fn* in the oral cavity, HSC-3 cells were infected with *Fn* at a multiplicity of infection (MOI; Number of bacteria

per one cell) of 1000 twice a week for a 4-week period at 37 ℃ with 5 % $CO_2$ in a 10 cm dish. Specifically, cells were seeded at $1.0\times10^6$ cells in a 10 cm dish and incubated for 24 h to allow the cells to adhere to the plate. After 24 h, *Fn* was mixed with MEM complete without antibiotics to achieve a MOI of 1000, which was replaced with the medium of the aforementioned cells after washing the wells three times with PBS. This was repeated every three or four days. During this period, cells that stopped proliferating under *Fn* exposure were removed by trypsin treatment (data not shown), whereas other proliferating cells were continually exposed to *Fn* infection. Cell shapes were observed using phase-contrast microscopy. In some experiments, cells were infected with or without *Fn* for four weeks in the presence of dexamethasone (DEX, an NF-κB inhibitor).

**2.4 Cell counting Kit-8 (CCK-8) assay**

Cells were seeded in a 96-well plate at a rate of 5,000 cells per well and incubated for 24 h. A 10 % CCK-8 solution was added to each well and incubated for 2 h. The absorbance of the colored solution was measured at 450 nm using a microplate reader (iMark Microplate Reader; Bio-Rad, Hercules, US). Three replicate wells for each group were set up in triplicates and a culture medium without cells was used as a negative control.

**2.5 Wound-healing assay**

Cells were seeded in a 6-well plate at a rate of $5.0\times10^5$ cells/well and grown until confluence. A linear wound was created by scratching at the center of each well using a 1000 μL pipette tip, and the wound closure at the same site was observed after 6, 12, 18, and 24 h under a phase-contrast microscope (BZ-X800;

KEYENCE, Tokyo, JP) at 10× magnification. The images were analyzed using IMAGE J software (National Institutes of Health, Bethesda, MD, US). Three replicate wells were set up for each group, and the experiment was conducted in triplicate. Wound closure (%) was calculated by the following equation: Wound closure (%) = [Total vacant area (0 h) − Total vacant area (X h)]/Total vacant area (0 h) × 100.

**2.6 Transwell migration assay**

Cells ($1.0\times10^4$ cells/ chamber) were seeded in 300 μL of a serum-free medium on the upper chamber (Transparent PET, Membrane 24 Well 8.0 μm pore size; FALCON, Durham, USA), and 600 μL of MEM complete was added in the lower chamber. After 24 h of incubation, cells on the top surface of the filter were removed by swabbing. Cells were stained with 2 % crystal violet, and cell migration through the pores to the lower surface was recorded under a microscope (TF50-B; Kenis, Osaka, JP). The images obtained were analyzed using IMAGE J software. Three replicate wells were set up for each group, and the experiment was conducted in triplicate.

**2.7 Western Blotting**

Each cell lysate was collected and separated by sodium dodecyl sulfate-polyacrylamide gel electrophoresis. The proteins were then transferred to polyvinylidene fluoride membranes, and the molecules related to EMT were detected. The primary antibodies used were as follows: anti-β-actin (clone AC15) (1:5000) (Sigma-Aldrich), Purified anti-human CD324 (E-cadherin) (1:1000) (Bio-Legend, San Diego, US), Purified anti-CD325 (N-cadherin) (1:1000) (Bio-Legend), Purified anti-cytokeratin (pan reactive) (1:1000) (Bio-

Legend), snail (C15 D3) rabbit mAb (1:1000) (Cell Signaling Technologies). Protein bands were detected using appropriate second antibodies and Luminata Forte Western HRP Substrate (Millipore Sigma, Darmstadt, Germany), then analyzed using LAS-1000 (Fujifilm, Tokyo, JP).

**2.8 Real-time RT-PCR**

Total RNA was extracted using the ReliaPrep RNA Miniprep System (Promega, Madison, WI, US), and cDNA was synthesized from 1 μg of total RNA using the Revertra Ace qPCR Master Mix with gDNA Remover (TOYOBO). Real-time PCR was performed using a CFX Opus 96 (Bio-Rad) with cDNA prepared using the KOD SYBR qPCR Mix (TOYOBO). Reactions were performed as follows: 98 ℃ for 2 min, followed by 40 cycles of 98 ℃ for 10 s, 65 ℃ for 10 s, and 98 ℃ for 30 s. The primer sequences used are as follows: β-actin: 5'-GGCCAACCGCGAGAAGAT-3' (forward), and 5'-CGTCACCGGAGTCCATCA-3' (reverse), CD44; 5'-TGAATATAACCTGCCGCTTTG-3' (forward), and 5'-GCTTTCTCCATCTGGGCCAT-3' (reverse), CD133; 5'-GAGTCGGAAACTGGCAGATAGCA-3' (forward), and 5'-ACGCCTTGTCCTTGGTAGTGTTG-3' (reverse). Three replicate wells were set up for each group, and the experiment was conducted in triplicate. Each value was evaluated using the ΔΔCT method.

**2.9 Statistical analysis**

All data were obtained from at least three separate experiments. Statistical differences between groups were determined using Student's t-test. Statistical significance was set at $P<0.05$.

## 3. Results

### 3.1 Chronic *Fn* infection increases the proliferative capacity of HSC-3 cells in a time-dependent manner

The CCK-8 assay demonstrated a time-dependent increase in cell proliferation following *Fn* infection. Cell proliferation at 4-week and 2-week infections significantly differed from that without infection. Moreover, the cell proliferation rate at 4-week infection was significantly different from that at 2-week infection (Fig.1).

### 3.2 Chronic *Fn* infection increases the invasive and migratory capacities of HSC-3 cells in a time-dependent manner

The wound-healing assay showed that wound closure was promoted in a time-dependent manner after *Fn* infection. Six hours after scratching, the wound closure level at the 4-week infection was significantly different from that with no infection. Twelve hours after scratching, the wound closure levels at 4-week and 2-week infection were significantly different from those with no infection. In addition, the wound closure level at 4-week infection was significantly different from that at 2-week infection. Eighteen hours after scratching, wound closure levels at 4-week and 2-week infection were significantly different from those with no infection (Fig.2a, b). The results of the transwell migration assay showed that the average migration area increased in a time-dependent manner after *Fn* infection. The average migration area of the 4-week infection group was significantly different from that of the no infection group. Additionally, the average migration area of the 4-week infection group significantly differed from

that of the 2-week infection group (Fig.2c, d).

### 3.3 Chronic *Fn* infection induces a time-dependent decrease in epithelial markers and a time-dependent increase in mesenchymal markers in HSC-3 cells

It was found that the expression levels of the epithelial markers E-cadherin and Cytokeratin were downregulated in a time-dependent manner, whereas those of the mesenchymal markers N-cadherin and Snail were upregulated by Western blotting (Fig.3).

### 3.4 Chronic *Fn* infection induces time-dependent EMT in HSC-3 cells

Phase-contrast microscopy images of HSC-3 cells after 4-week, 2-week, and no infection revealed that *Fn* infection induced a time-dependent transformation into a slender and elongated morphology, along with cell-to-cell separation (Fig.4). This suggests loss of cell polarity and intercellular adhesion. In addition, rod-shaped *Fn* particles were observed around the cells, suggesting that these cells were affected by *Fn*. Taken together, chronic *Fn* infection induced a time-dependent EMT in HSC-3 cells, as indicated by increased proliferative, invasive, and migratory capacities, decreased expression of epithelial markers, and increased expression of mesenchymal markers in HSC-3.

### 3.5 Chronic *Fn* infection induces HSC-3 cells to acquire cancer stem cell-like properties in a time-dependent manner

Since HSC-3 cells acquire the characteristics of mesenchymal cells and may have acquired the properties of cancer stem cells through chronic *Fn* infection, the expression levels of CD44 and CD133, which are markers of cancer stem cells, were analyzed using real-time RT-PCR. The mRNA level of CD44 was

upregulated in a time-dependent manner, and the mRNA level at 4-week infection was significantly different from that at no infection. Although no significant differences were observed, the mRNA level of CD133 tended to be upregulated in a time-dependent manner (Fig.5).

### 3.6 DEX impairs EMT of HSC-3 cells induced by chronic *Fn* infection

HSC-3 cells were infected with or without *Fn* for four weeks in the presence of DEX (50, 100, and 200 nM). In the presence of DEX, HSC-3 cells did not show any trend toward increased proliferative, invasive, or migratory capacities (Fig.6a, b, c, d), and there were no significant changes in the levels of E-cadherin, cytokeratin, N-cadherin, or Snail (Fig.6e). In addition, no transformation into a slender or elongated morphology, or cell-to-cell separation were observed (Fig.6f). Taken together, DEX treatment inhibited EMT in HSC-3 cells induced by chronic *Fn* infection.

## 4. Discussion

The effects of chronic inflammation on tumors by *Fn* were confirmed in this study. To our knowledge, this is the first study to examine the effects of chronic *Fn* infection on oral tumor cells. In this study, EMT was induced in a time-dependent manner, even after chronic *Fn* infection, suggesting that oral cancer cells continue to be adversely affected by chronic *Fn* infection. Routine decontamination of the oral cavity to prevent chronic *Fn* infection may be important for controlling tumor invasion and metastasis.

CD44 is known as a cancer stem cell marker for squamous cell carcinoma of the head and neck[23], and its mRNA level is significantly and time-dependently

elevated by *Fn* infection in this study. These findings indicate that cells subjected to chronic *Fn* infection have poor prognostic properties, including increased cell proliferative capacity, invasive potential, and acquisition of mesenchymal cell characteristics. CD133 is reported to be a cancer stem cell marker found in several cancers [24], although a failure to detect its positivity in oral cancer has also been reported[25]. In this study, the mRNA level of CD133 tended to increase in a time-dependent manner, suggesting the possibility that the cells might acquire cancer stem cell characteristics.

Studies on colon cancer cells have reported that *Fn* promotes EMT by inducing Annexin A1 and activating the Wnt/β-catenin signaling pathway through FadA and E-cadherin [12,13]. Additionally, it has been observed that *Fn* activates the Toll-like receptor (TLR)4/ MyD88/NF-κB pathway, leading to the promotion of EMT [14–16] and chemotherapy resistance [17].

In the case of oral cancer cells, studies have reported that *Fn* suppresses apoptosis by activating the Wnt5a/NFAT pathway and promoting the migration of oral cancer cells, resulting in cisplatin resistance [26]. Thus, the mechanism may be similar to that of colon cancer cells. *Fn* infection activates the JAK-STAT pathway via TLRs to regulate the expression of genes that promote cell proliferation, angiogenesis, metastasis, and invasion, thereby promoting cancer progression[27].

In contrast to the JAK-STAT pathway, PI3K and its downstream pathways have been reported less frequently. Therefore, we used DEX to investigate the association between JAK-STAT and their downstream pathway, the PI3K pathway, in oral cancer. NF-κB is known to be upregulated by activation of the PI3K pathway. According to Janeway's IMMUNOBIOLOGY, DEX binds to an intracellular steroid

receptor and its complex directly interacts with NF-κB, thereby inhibiting transcription of its downstream genes [28]. Only a few studies have reported an association between DEX administration and malignancies. A previous study reported that DEX inhibits hypoxia-induced EMT in colon cancer cells [29]. Furthermore, DEX improves partial EMT in oral cancer when administered to cells undergoing EMT [30]. Similarly, EMT was inhibited by DEX treatment in this study. This may suggest that the PI3K pathway is associated with EMT induced by *Fn* infection in oral cancer, as well as its upstream JAK-STAT pathway. Therefore, inhibition of the JAK-STAT pathway and the PI3K pathway may inhibit malignant tumor progression. However, the detail mechanism of EMT has not been investigated, and further studies on the association between the JAK-STAT pathway and PI3K pathway are required.

In this study, the effects of chronic *Fn* infection were examined using one cell line, HSC-3 cells, and further studies using clinical specimens will be needed in the future.

## 5. Conclusions

To our knowledge, this is the first study to show that chronic *Fn* infection induces EMT in HSC-3 cells in a time-dependent manner. In addition, HSC-3 cells may acquire cancer stem cell characteristics in a time-dependent manner following chronic *Fn* infection. Furthermore, it was suggested that the JAK-STAT pathway is involved in the *Fn*-induced EMT, since the EMT induction was inhibited by DEX treatment.

## Reference


[1] Bray F, Ferlay J, Soerjomataram I, Siegel RL, Torre LA, Jemal A. Global cancer statistics 2018: GLOBOCAN estimates of incidence and mortality worldwide for 36 cancers in 185 countries. CA Cancer J Clin 2018;68:394–424.

[2] Ling Z, Cheng B, Tao X. Epithelial-to-mesenchymal transition in oral squamous cell carcinoma: Challenges and opportunities. Int J Cancer 2021;148:1548–61.

[3] Azca A, Yeh JJ, Sandler RS, Mccoy AN, Keku TO. *Fusobacterium* Is Associated with Colorectal Adenomas. PLoS One. 2013;8:e53653.

[4] Hsieh Y, Tung S, Pan H, Yen C, Xu H. Increased Abundance of *Clostridium* and *Fusobacterium* in Gastric Microbiota of Patients with Gastric Cancer in Taiwan. Sci Rep 2018;8:158.

[5] Mitsuhashi K, Nosho K, Sukawa Y, Matsunaga Y. Association of *Fusobacterium species* in pancreatic cancer tissues with molecular features and prognosis. Oncotarget. 2015;6:7209-20.

[6] Signat B, Roques C, Poulet P, Duffaut D. Role of *Fusobacterium nucleatum* in periodontal health and disease. Curr Issues Mol Biol 2011;13:25–36.

[7] Hooper SJ, Crean SJ, Lewis MAO, Spratt DA, Wade WG, Wilson MJ. Viable bacteria present within oral squamous cell carcinoma tissue. J Clin Microbiol 2006;44:1719–25.

[8] Pushalkar S, Ji X, Li Y, Estilo C, Yegnanarayana R, Singh B, et al. Comparison of oral microbiota in tumor and non-tumor tissues of patients with oral squamous cell carcinoma. BMC Microbiol 2012;12:144.

[9] Lara-Tejero M, Galan JE. A bacterial toxin that controls cell cycle progression as a deoxyribonuclease I-like protein. Science 2000;290:354–7.

[10] Galvão-Moreira LV, Da Cruz MCFN. Oral microbiome, periodontitis and risk of head and neck cancer. Oral Oncol 2016;53:17–9.

[11] Karmakar S, Kar A, Thakur S, Rao VUS. Periodontitis and oral Cancer-A striking link. Oral Oncol 2020;106:104630.

[12] Rubinstein MR, Baik JE, Lagana SM, Han RP, Raab WJ, Sahoo D, et al. *Fusobacterium nucleatum* promotes colorectal cancer by inducing Wnt/β-catenin modulator Annexin A1. EMBO Rep 2019;20:e47638.

[13] Rubinstein MR, Wang X, Liu W, Hao Y, Cai G, Han YW. *Fusobacterium nucleatum* promotes colorectal carcinogenesis by modulating E-cadherin/β-catenin signaling via its FadA adhesin. Cell Host Microbe 2013;14:195–206.

[14] Yu MR, Kim HJ, Park HR. *Fusobacterium nucleatum* Accelerates the Progression of Colitis-Associated Colorectal Cancer by Promoting EMT. Cancers(Basel) 2020;12:2728.

[15] Yang Y, Weng W, Peng J, Hong L, Yang L, Toiyama Y, et al. *Fusobacterium nucleatum* Increases Proliferation of Colorectal Cancer Cells and Tumor Development in Mice by Activating Toll-Like Receptor 4 Signaling to Nuclear Factor−κB, and Up-regulating Expression of MicroRNA-21. Gastroenterology 2017;152:851–866.e24.

[16] Kong C, Yan X, Zhu Y, Zhu H, Luo Y, Liu P, et al. *Fusobacterium Nucleatum* Promotes the Development of Colorectal Cancer by Activating a Cytochrome P450/Epoxyoctadecenoic Acid Axis via TLR4/Keap1/NRF2 Signaling. Cancer Res 2021;81:4485–4498.

[17] Yu T, Guo F, Yu Y, Sun T, Han J, Kryczek I, et al. *Fusobacterium nucleatum* Promotes Chemoresistance to Colorectal Cancer by Modulating Autophagy. Cell

2017;170:548–63.e16.

[18] Abdulkareem AA, Shelton RM, Landini G, Cooper PR, Milward MR. Periodontal pathogens promote epithelial-mesenchymal transition in oral squamous carcinoma cells in vitro. Cell Adh Migr 2018;12:127–37.

[19] Abdulkareem AA, Shelton RM, Landini G, Cooper PR, Milward MR. Potential role of periodontal pathogens in compromising epithelial barrier function by inducing epithelial-mesenchymal transition. J Periodontal Res 2018;53:565–74.

[20] Zhang S, Li C, Liu J, Geng F, Shi X, Li Q, et al. *Fusobacterium nucleatum* promotes epithelial-mesenchymal transiton through regulation of the lncRNA MIR4435-2HG/miR-296-5p/Akt2/SNAI1 signaling pathway. FEBS J 2020;287:4032–47.

[21] Shao W, Fujiwara N, Mouri Y, Kisoda S, Yoshida K, Yoshida K, et al. Conversion from epithelial to partial-EMT phenotype by *Fusobacterium nucleatum* infection promotes invasion of oral cancer cells. Sci Rep 2021;11:14943.

[22] Harrandah AM, Chukkapalli SS, Bhattacharyya I, Progulske-Fox A, Chan EKL. *Fusobacteria* modulate oral carcinogenesis and promote cancer progression. J Oral Microbiol 2020;13:1849493.

[23] Prince ME, Sivanandan R, Kaczorowski A, Wolf GT, Kaplan MJ, Dalerba P, et al. Identification of a subpopulation of cells with cancer stem cell properties in head and neck squamous cell carcinoma. Proc Natl Acad Sci U S A 2007;104:973–8.

[24] Zhang Q, Shi S, Yen Y, Brown J, Ta JQ, Le AD. A subpopulation of CD133+ cancer stem-like cells characterized in human oral squamous cell carcinoma confer resistance to chemotherapy. Cancer Lett 2010;289:151–60.

[25] Mărgăritescu C, Pirici D, Simionescu C, Stepan A. The utility of CD44, CD117

and CD133 in identification of cancer stem cells (CSC) in oral squamous cell carcinomas (OSCC). Rom J Morphol Embryol 2012;52:985–93.

[26] Da J, Wang X, Li L, Xu Y. *Fusobacterium nucleatum* Promotes Cisplatin-Resistance and Migration of Oral Squamous Carcinoma Cells by Up-Regulating Wnt5a-Mediated NFATc3 Expression. Tohoku J Exp Med 2021;253:249–59.

[27] Gallimidi AB, Fischman S, Revach B, Bulvik R, Rubinstein AM, Nussbaum G, et al. Periodontal pathgens *Porphyromonas gingivalis* and *Fusobacterium nucleatum* promote tumor progression in an oral-specific chemical carcinogenesis model. Oncotarget 2015;6:22613–23.

[28] Murphy K, Travers P, Walport M. JANEWAY'S IMMUNOBIOLOGY. 7th ed. New York: Garland Science; 2008.

[29] Kim JH, Hwang YJ, Han SH, Lee YE, Kim S, Kim YJ, et al. Dexamethasone inhibits hypoxia-induced epithelial-mesenchymal transition in colon cancer. World J Gastroenterol 2015;21:9887–99.

[30] Okuda S, Yamakado N, Higashikawa K, Uetsuki R, Ishida F, Rizqiawan A, et al. Dexamethasone resets stable association of nuclear Snail with LSD1 concomitant with transition from EMT to partial EMT. Biochem Biophys Reports 2022;30:101277.

**Fig.1**

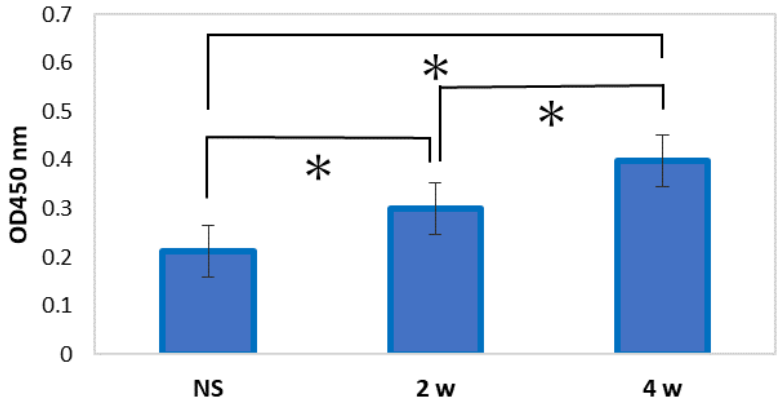


Cell proliferation of HSC-3 cells at 4-week, 2-week, and no infection. ＊P<0.05

**Fig.2**

**(a)**

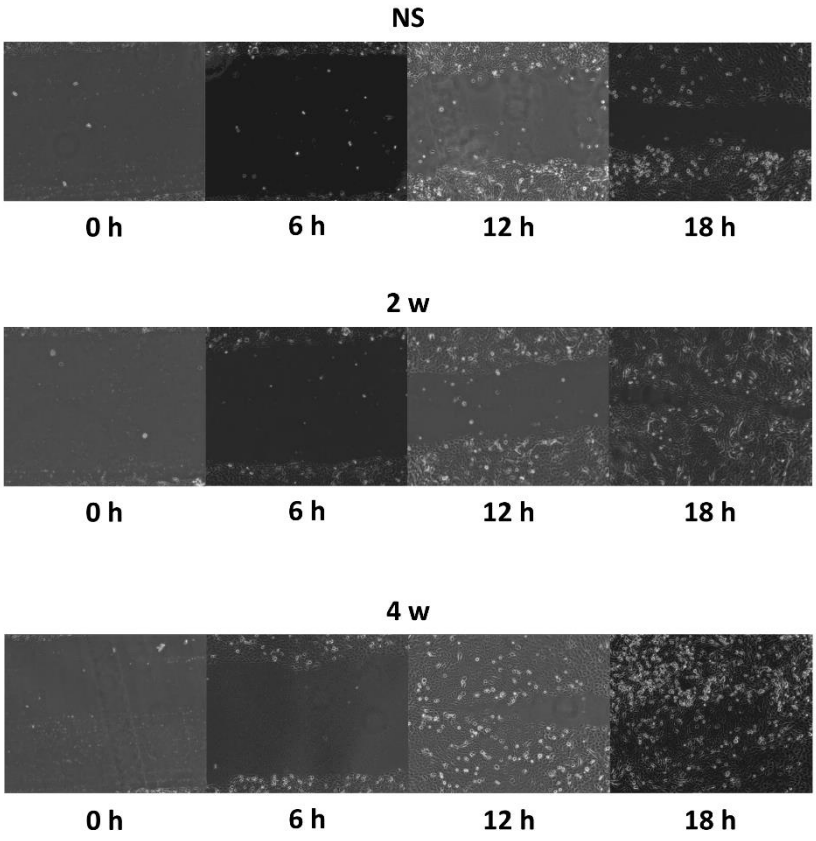

**(b)**

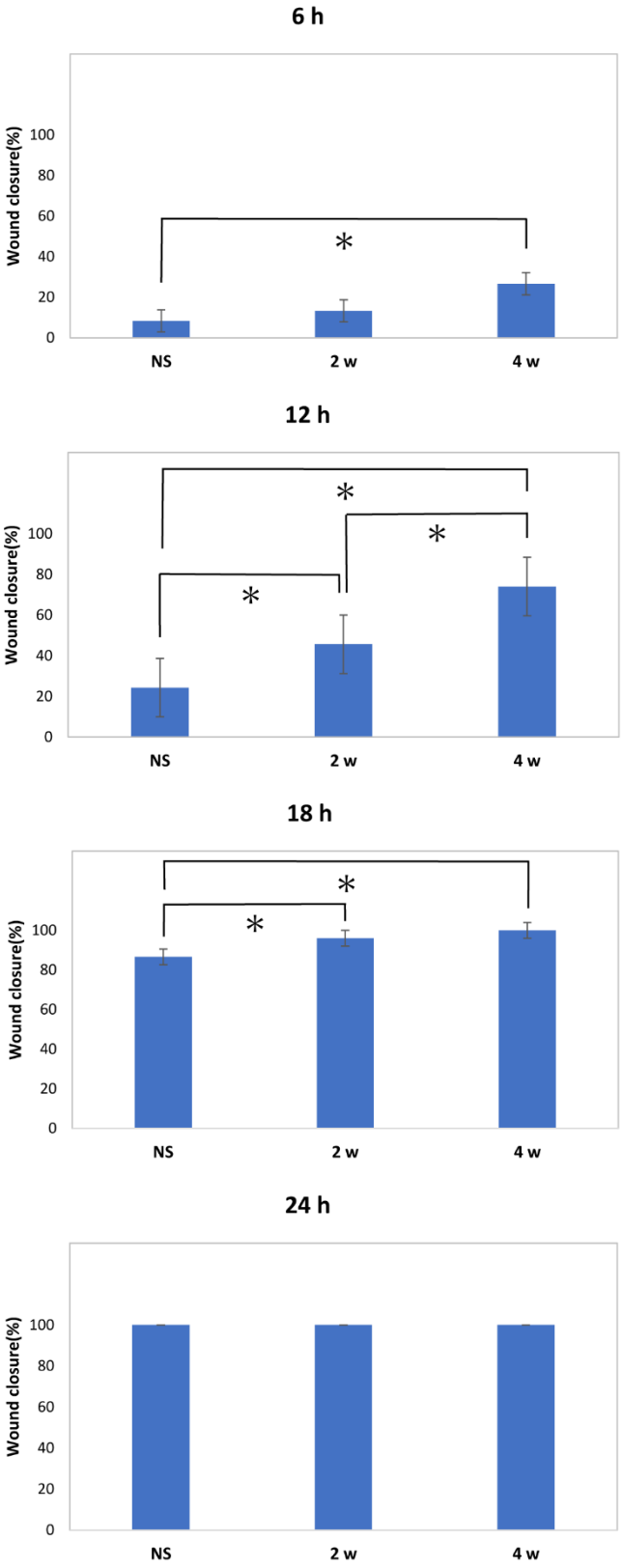
6 h
Wound closure(%)
100
80
60
40
20
0
*
NS
2 w
4 w
12 h
Wound closure(%)
100
80
60
40
20
0
*
*
*
NS
2 w
4 w
18 h
Wound closure(%)
100
80
60
40
20
0
*
*
NS
2 w
4 w
24 h
Wound closure(%)
100
80
60
40
20
0
NS
2 w
4 w

**(c)**

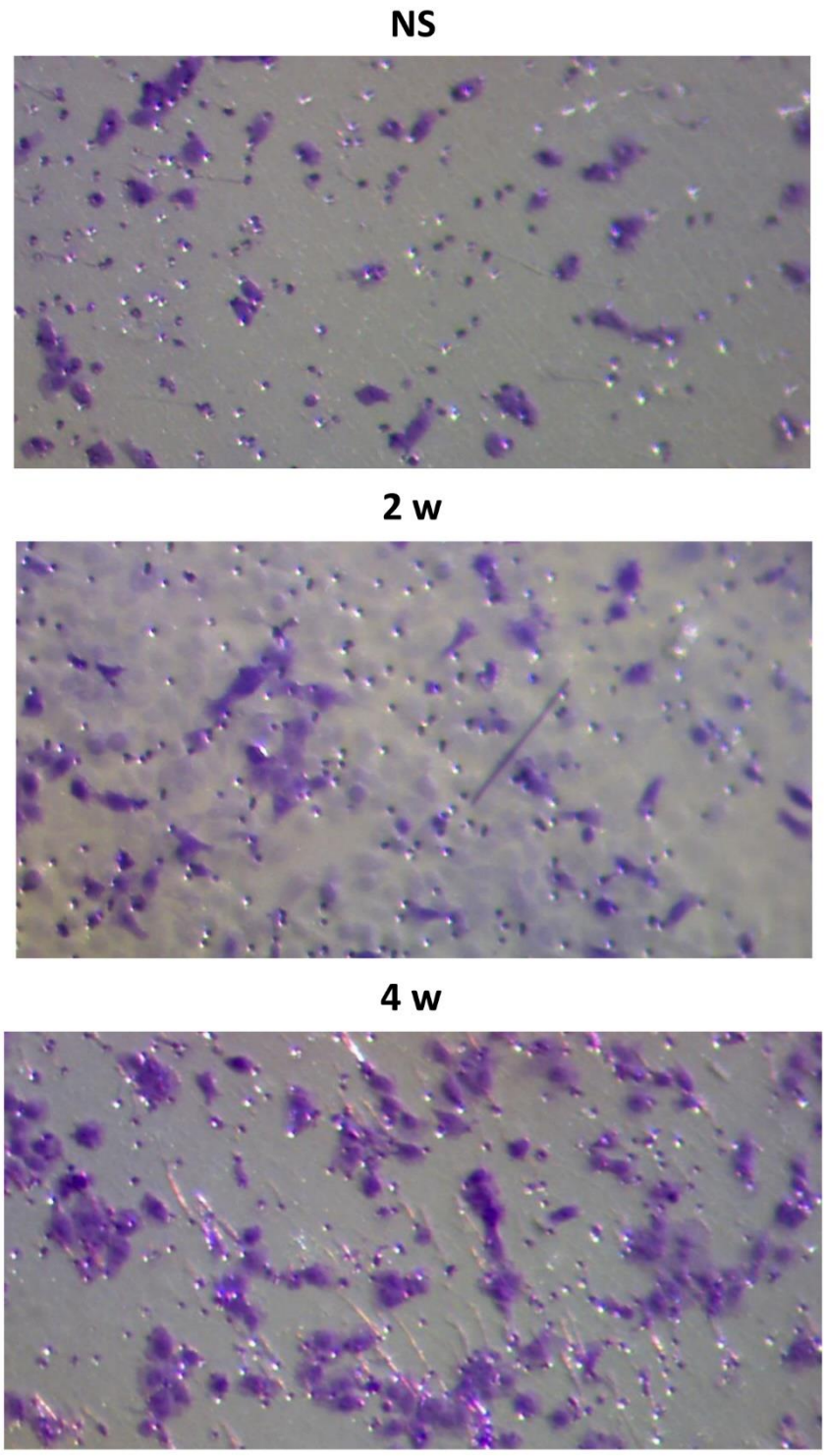

**(d)**

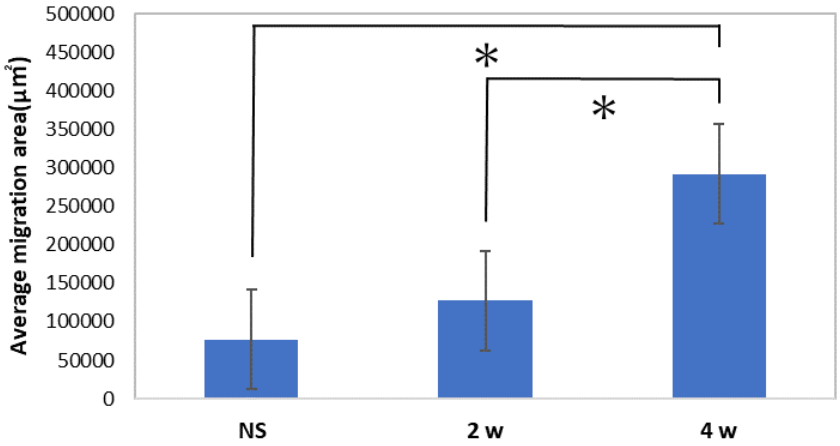


(a) Representative images of wound healing assay recorded at 0, 6, 12, and 18 h after scratching in HSC-3 cells at 4-week, 2-week, and no infection at 10× magnification under a phase-contrast microscope. (b) Wound closure (%) at 6 h, 12 h, 18 h, and 24 h in HSC-3 cells at 4-week, 2-week, and no infection. ＊P<0.05 (c) Representative images of transwell migration assay recorded at 24 h after seeding HSC-3 cells at 4-week, 2-week, and no infection at 30× magnification under a microscope. (d) Average migration area （μ ㎡） at 24 h for HSC-3 at 4-week, 2-week, and no infection. ＊P<0.05

**Fig.3**

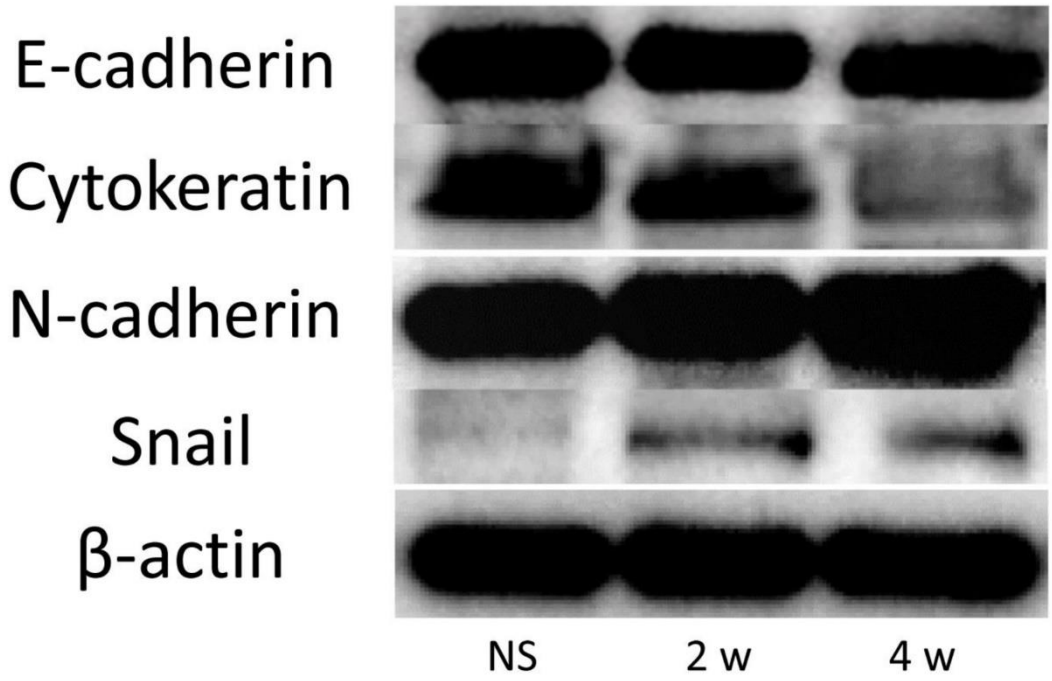


Western blot images of HSC-3 cells at 4-week, 2-week, and no infection.

**Fig.4**

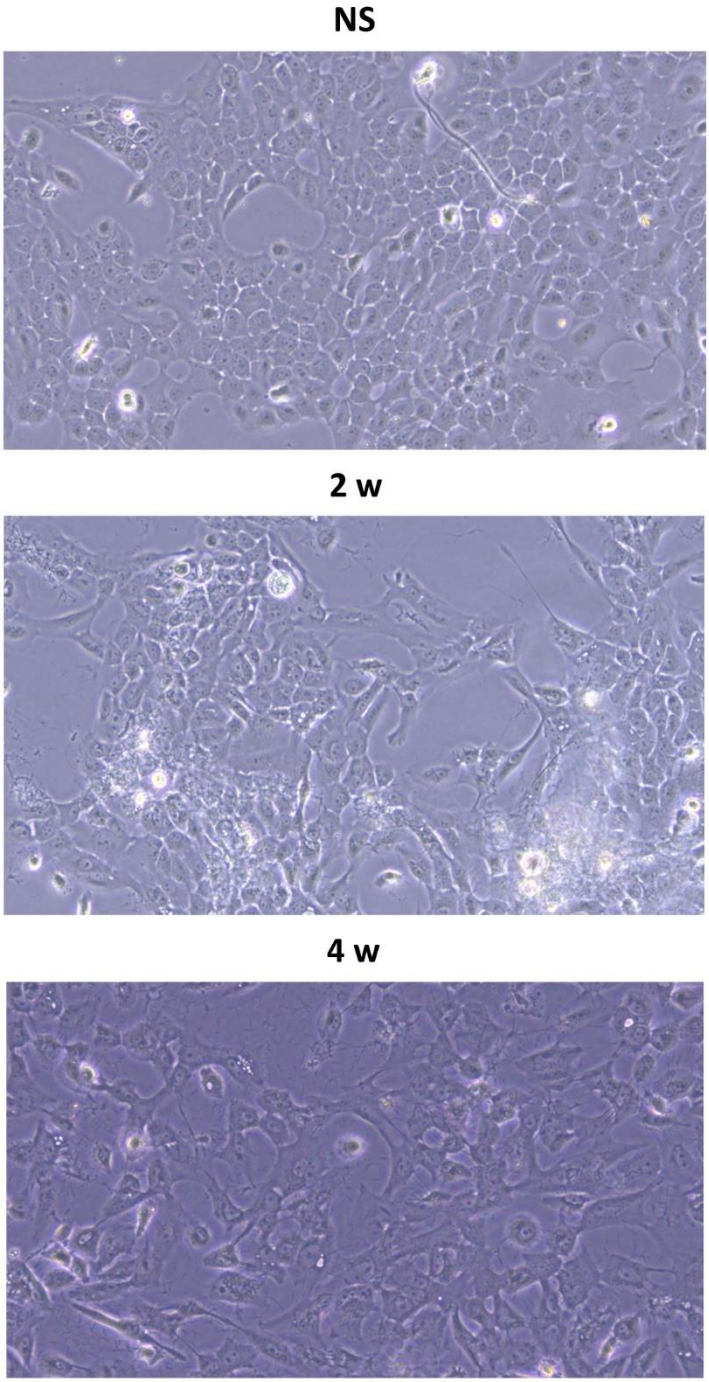


Representative images of HSC-3 cells at 4-week, 2-week, and no infection under a phase-contrast microscope.

**Fig.5**

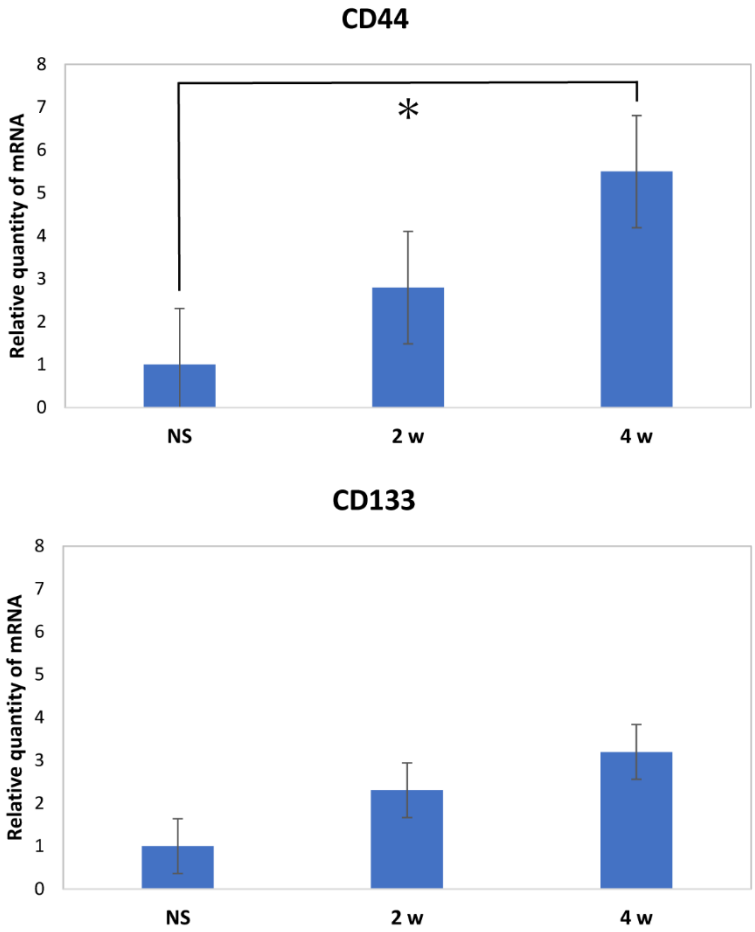


mRNA level of CD44, CD133 of HSC-3 cells at 4-week, 2-week, and no infection measured by real-time RT-PCR. ＊P<0.05

**Fig.6**

**(a)**

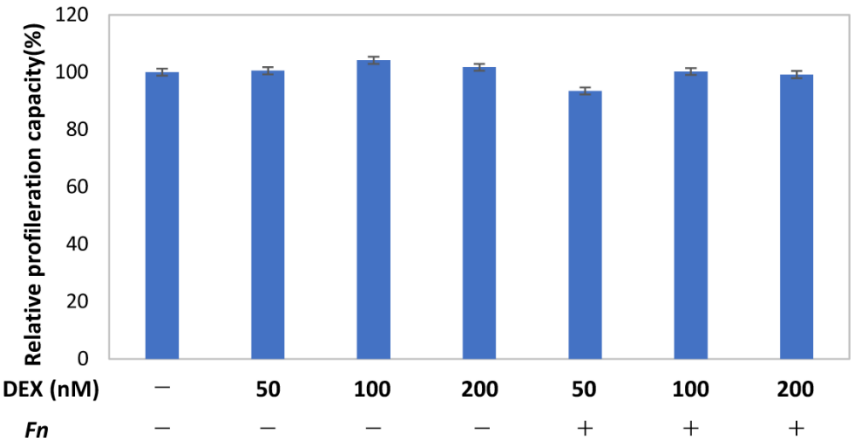
Relative profileration capacity(%)
120
100
80
60
40
20
0
DEX (nM)
–
50
100
200
50
100
200
Fn
–
–
–
–
+
+
+

**(b)**

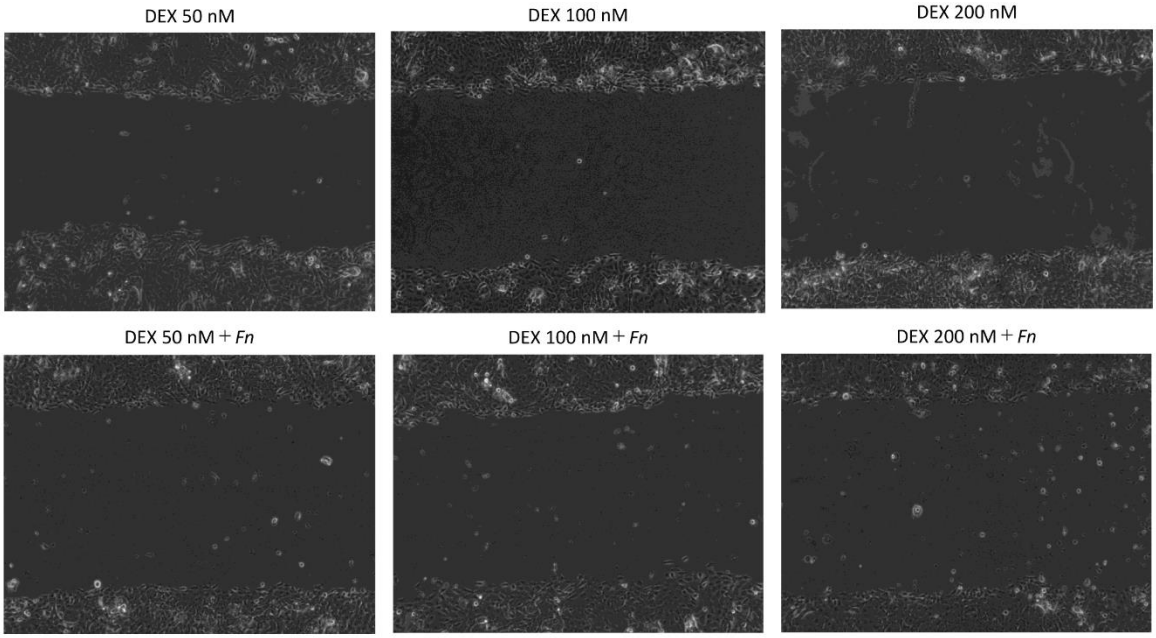
DEX 50 nM
DEX 100 nM
DEX 200 nM
DEX 50 nM + *Fn*
DEX 100 nM + *Fn*
DEX 200 nM + *Fn*

**(c)**

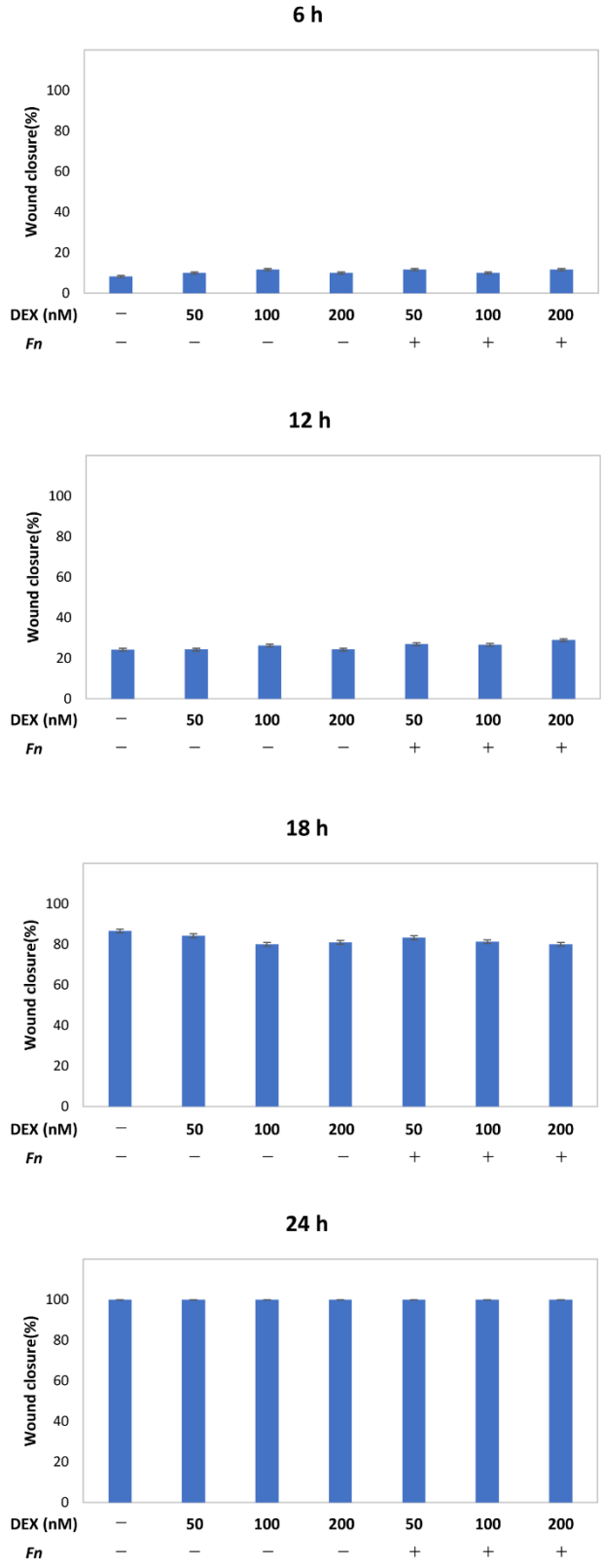
6 h
Wound closure(%)
100
80
60
40
20
0
DEX (nM) – 50 100 200 50 100 200
Fn – – – – + + +
12 h
Wound closure(%)
100
80
60
40
20
0
DEX (nM) – 50 100 200 50 100 200
Fn – – – – + + +
18 h
Wound closure(%)
100
80
60
40
20
0
DEX (nM) – 50 100 200 50 100 200
Fn – – – – + + +
24 h
Wound closure(%)
100
80
60
40
20
0
DEX (nM) – 50 100 200 50 100 200
Fn – – – – + + +

**(d)**

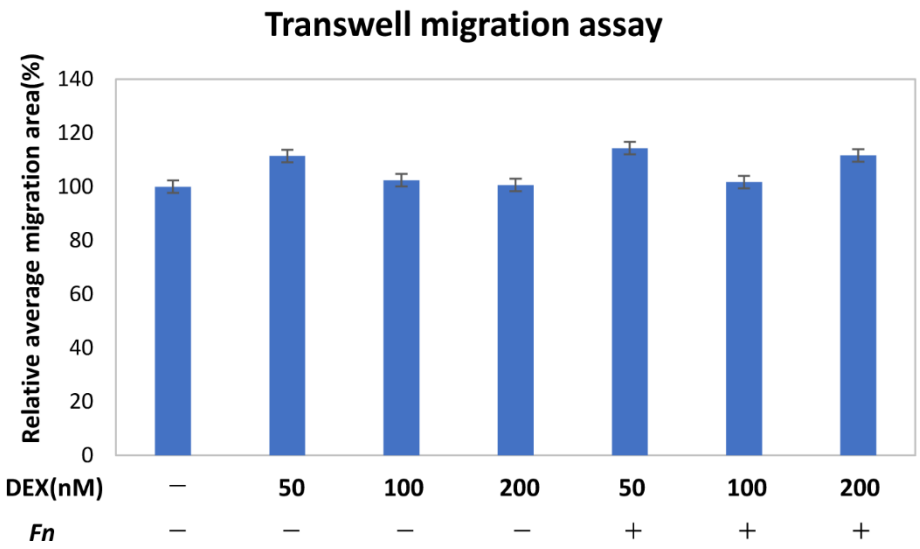
Transwell migration assay
Relative average migration area(%)
140
120
100
80
60
40
20
0
DEX(nM)
–
50
100
200
50
100
200
Fn
–
–
–
–
+
+
+

**(e)**

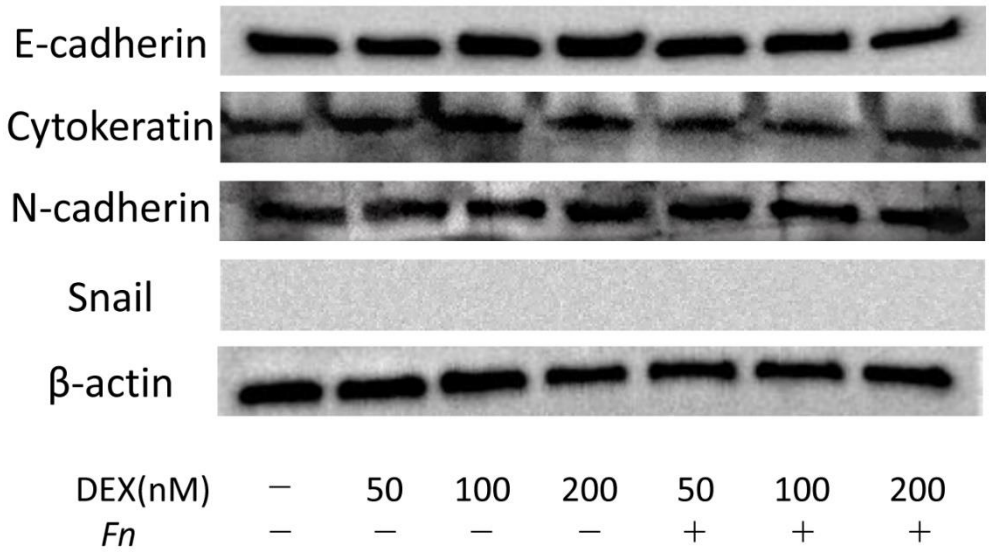
E-cadherin
Cytokeratin
N-cadherin
Snail
β-actin
DEX(nM) − 50 100 200 50 100 200
*Fn* − − − − + + +

**(f)**

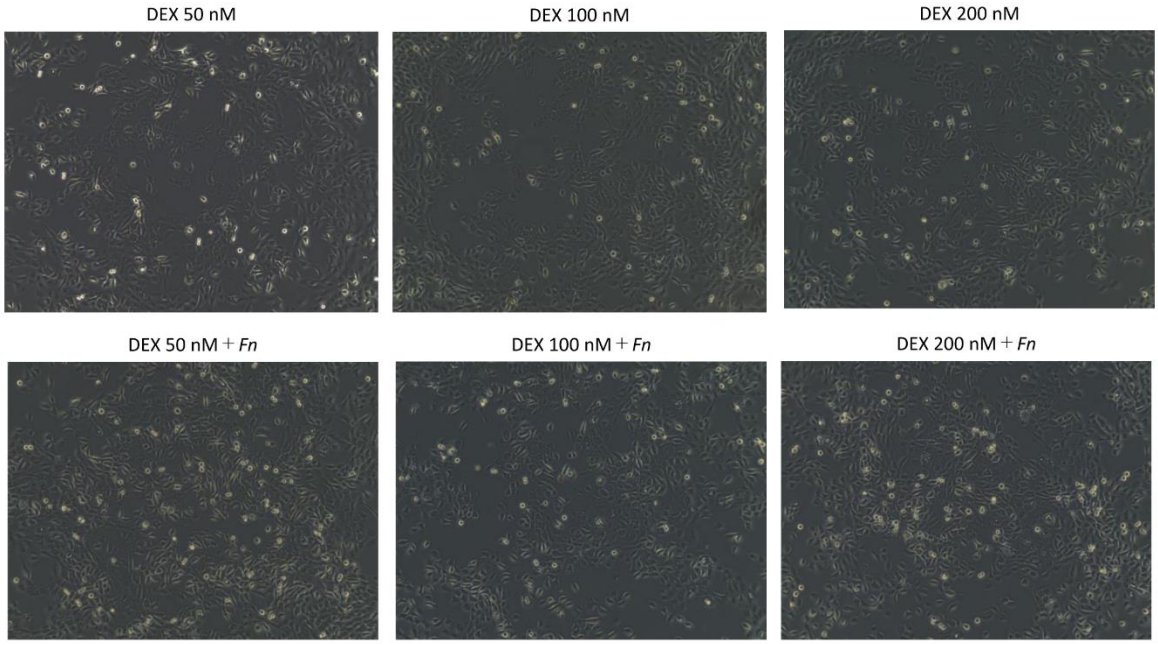


(a) Comparison of cell proliferation of HSC-3 cells with DEX, DEX and *Fn*, with that of no infection (%). (b) Representative images of wound healing assay recorded at 12 h after scratching in HSC-3 cells with DEX, DEX and *Fn*, and no infection at 10× magnification under a phase-contrast microscope. (c) Wound closure (%) at 6 h, 12 h, 18 h, and 24 h for HSC-3 cells with DEX, DEX and *Fn*, and no infection. (d) Comparison of average migration area of HSC-3 cells with DEX, DEX and *Fn,* with that of no infection (%). (e) Western blot images of HSC-3 cells with DEX, DEX and *Fn*, and no infection. (f) Representative images of HSC-3 cells with DEX, DEX and *Fn*, and no infection under a phase-contrast microscope.